NASA TECHNICAL NOTE

NASA TN D-2530


NASA TN D-2530



# PRELAUNCH ANALYSIS OF HIGH ECCENTRICITY ORBITS

*by Barbara E. Shute*

*Goddard Space Flight Center*
*Greenbelt, Md.*

NATIONAL AERONAUTICS AND SPACE ADMINISTRATION • WASHINGTON, D. C. • DECEMBER 1964

# PRELAUNCH ANALYSIS OF HIGH ECCENTRICITY ORBITS

By Barbara E. Shute

Goddard Space Flight Center
Greenbelt, Md.

NATIONAL AERONAUTICS AND SPACE ADMINISTRATION

For sale by the Office of Technical Services, Department of Commerce,
Washington, D.C. 20230 -- Price $2.00

# PRELAUNCH ANALYSIS OF HIGH ECCENTRICITY ORBITS

by
Barbara E. Shute
*Goddard Space Flight Center*

SUMMARY

This paper surveys the prelaunch analyses of high eccentricity earth orbits. Pertinent two-body calculations are presented and computer programs for the perturbations on high eccentricity earth orbits are reviewed. Graphs of the results of numerical integration are used to illustrate variations in the orbital elements due to the perturbing forces of the earth's atmosphere and oblateness, and to the gravitational fields of the moon and sun. Auxiliary calculations that are useful to the experimenters are discussed. The selection of a launch time to meet experimenters' requirements for the orbital lifetime and spacecraft environment is demonstrated by the construction of a launch window map.

CONTENTS

## List of Symbols

### ELLIPTIC ELEMENTS

| | |
|---|---|
| $a$ | semimajor axis |
| $e$ | eccentricity |
| $i$ | inclination |
| $\omega$ | argument of perigee |
| $\Omega$ | right ascension of the ascending node |
| $\nu$ | true anomaly |
| $A$ | apogee distance from the earth's center |
| $P$ | perigee distance from the earth's center |
| $T$ | orbital period |
| $n$ | mean motion |
| $v_A$ | velocity at apogee |
| $v_P$ | velocity at perigee |
| $E$ | eccentric anomaly |
| $t$ | time since perigee passage |
| $r$ | radial distance to a satellite |

### POLAR COORDINATES (measured with respect to a fixed earth)

| | |
|---|---|
| $r$ | distance from the earth's center |
| $\phi$ | latitude |
| $\lambda$ | longitude |
| $v$ | velocity magnitude |
| $z$ | velocity azimuth (measured clockwise from the north) |
| $\gamma$ | elevation angle (flight path angle) |

### CONSTANTS

| | |
|---|---|
| $GM$ | product of the universal gravitational constant and the earth's mass |
| $GM_m$ | product of the universal gravitational constant and the moon's mass |
| $J$ | coefficient of the earth's second harmonic |

### EXPERIMENT PARAMETERS

| | |
|---|---|
| $\alpha$ | angle between the spin axis and the solar direction |
| $\beta$ | angle between the spin axis and the ecliptic |
| $R_e$ | earth's radius |

### RELATION BETWEEN EARTH-FIXED AND INERTIAL COORDINATES

| | |
|---|---|
| $\psi$ | sidereal time or Greenwich hour angle of the vernal equinox given in hours, minutes, seconds |

# PRELAUNCH ANALYSIS OF HIGH ECCENTRICITY ORBITS

by
Barbara E. Shute
*Goddard Space Flight Center*

## INTRODUCTION

NASA has scheduled several series of scientific satellites with high eccentricity orbits ($e > 0.8$) including S-3*, the Eccentric Geophysical Observatories (EGO), and the Interplanetary Monitoring Platforms (IMP). Prelaunch orbital analyses are being performed to provide advance knowledge on parameters significant to the performance of the experiments, and to aid in the selection of orbits which satisfy the criteria imposed by the experiments. Two basic types of calculations may be distinguished: (1) projecting the dynamical future of the orbit; (2) calculating, from the orbital trajectory, auxiliary quantities (usually related to the position of the sun) which reflect the performance of experiments or batteries.

The orbital parameters for high eccentricity orbits are less stable than those for the extensively considered circular orbits. Orbital lifetimes are critically affected by solar and lunar gravitational forces acting on the orbit. In extreme cases the gravitation of the moon may lower the perigee from an initial height of 300 km to ground level in one or two orbits. The inclination of an orbit also may exhibit large shifts; in one extreme case for IMP the initial inclination of 33 deg is pushed to 90 deg in about a year.

Auxiliary quantities are calculated that are pertinent to an experiment or to the functioning of an experiment system. The time a satellite spends in the shadow of the earth may be substantial, and during this time the solar cells will not be charging the batteries. The location of the apogee may be selected for the investigation of particles in particular regions with respect to the earth's magnetic field, solar plasma, etc. The angle between a satellite's axis of rotation and the sun, the "spin-axis sun angle" or the "solar aspect," determines the amount of sunlight falling on different portions of an experiment. This angle may be calculated as a function of time from the injection conditions only; usually auxiliary quantities must be derived from the projected history of the orbit.

The most feasible way to select the above quantities uses the daily rotation of the earth. Under the assumption that the injection conditions with respect to the earth (latitude, longitude, height, azimuth, elevation angle, speed at burnout) are fixed, perigee may be placed anywhere on a parallel

*This is an internal designation used by Goddard Space Flight Center.

circle of latitude on the celestial sphere once every 24 hours. Those hours of the day when it is possible to inject a satellite so that the subsequent behavior of the quantities meets orbital and experimental specifications are known as a "launch window". Selection is made from calculations which assume many possible launch times. If all specifications are not met simultaneously, several solutions are available: (1) compromise of specifications; (2) payload revision; (3) revision of the trajectory to yield new injection conditions.

The actual computations of the orbital trajectories are made by sophisticated numerical integration computer programs. Several programs are available at present with varying capabilities for specific applications. The relative advantages and disadvantages are discussed in this report.

When computer results have been obtained, it is necessary to organize them into a logical and suitable form to prevent excess computation and to provide a convenient summary from which to select the most desirable orbits. The launch window map, which graphically portrays all suitable launch hours over an entire year, is the end result of such summaries.

The purpose of this paper is to delineate the problems of high eccentricity orbits and to summarize the state of the art of planning suitable orbits. The relative importance of gravitational perturbations and atmospheric drag is indicated. The effect of vehicle tolerance on the prediction of orbits and the subsequent lifetimes is shown. Computational accuracies are estimated by the comparison of results from different computer programs. Rough approximations are given where feasible. Data for the first satellite of the S-3 series, Explorer XII (1961 $\upsilon$1), launched on August 16, 1961, are compared with the theoretical computations.

## TWO-BODY CALCULATIONS

### S-3, EGO,and IMP Elements

The orbits discussed in this report refer to the three series of scientific satellites mentioned earlier–S-3, EGO, and IMP. The S-3 satellite weighs 83 lb and contains experiments to investigate the solar wind, the interplanetary magnetic field, and energetic particles. It is a spin-stabilized spacecraft with four solar-cell paddles. Of this series, Explorer XII and Explorer XIV (1962 $\beta\gamma$1) already have been launched into highly eccentric orbits. EGO is a 950 lb spacecraft in the Orbiting Geophysical Observatory series. It will carry experiments to study solar protons, trapped particles, cosmic rays, geomagnetic and interplanetary magnetic fields, micrometeorites, solar radio-noise bursts and the Gegenschein. IMP has a 125 lb payload to study the relationships of particle fluxes from the sun and the interplanetary magnetic field. It has a most eccentric orbit, to aid experimental measurements in cislunar space. The first satellite in this series has been launched as Explorer XVIII (1963 46A).

For reference and comparison three orbits to be used as examples are now presented: The nominal initial orbit of Explorers XII and XIV (S-3 and S-3A) is:

$$\begin{cases} a = 50{,}000 \text{ km} , \\ e = 0.867 , \\ i = 33.0 \text{ deg, and} \\ \omega = 153.5 \text{ deg} . \end{cases}$$

And $\Omega$ has each value between 0 and 360 deg once every 24 hours. The actual initial orbit of Explorer XII at launch, August 16, 1961, was:

$$\begin{cases} a = 45{,}000 \text{ km} , \\ e = 0.85 , \\ i = 33 \text{ deg} , \\ \omega = 153 \text{ deg, and} \\ \Omega = 171 \text{ deg} . \end{cases}$$

The nominal EGO orbit is:

$$\begin{cases} a = 62{,}000 \text{ km} , \\ e = 0.893 , \\ i = 30.8 \text{ deg, and} \\ \omega = -45.6 \text{ deg} . \end{cases}$$

The elements for a preliminary trajectory for the IMP series are:

$$\begin{cases} a = 145{,}000 \text{ km} , \\ e = 0.95 , \\ i = 33.0 \text{ deg, and} \\ \omega = 153.5 \text{ deg} . \end{cases}$$

The relative sizes and shapes of these orbits are compared in Figure 1.

As will be explained, the elements are not constant. The gravitational forces of the moon and sun and the oblateness of the earth interact in a complicated manner to disturb the orbit. The atmospheric drag may have an effect, depending on the height of perigee.

## Calculations Assuming Known Apogee and Perigee Distances

Often the initial apogee and perigee distances will be the first parameters specified. These imply the semimajor axis and the eccentricity:

$$A = \text{apogee distance} = a(1 + e) ,$$

$$P = \text{perigee distance} = a(1 - e) ,$$

where the apogee and perigee distances are taken from the center of the earth.

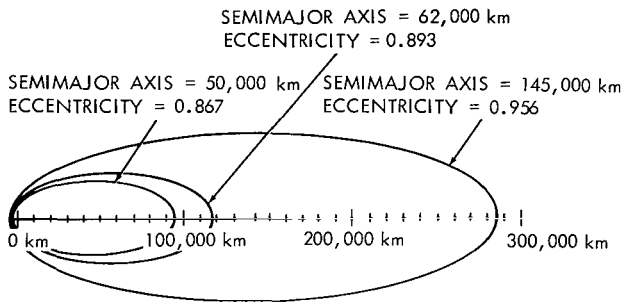


Figure 1—Comparison of S-3, EGO, and IMP orbits.

The period may be calculated from

$$T = \frac{2\pi a^{3/2}}{(GM)^{1/2}} ,$$

where GM is the gravitational attraction of the earth, whose current recommended value is 398603.2 $km^3/sec^2$ (Reference 1). The mean motion is

$$n = \frac{2\pi}{T}$$

As an example, the IMP orbit is calculated here under the assumptions that the apogee is 285,000 km (150,000 naut. mi.) from the surface or 291,000 km from the center of the earth, and the perigee is 204 km (110 naut. mi.) from the surface or 6598 km from the center of the earth. The following values are obtained:

$$a = \frac{A + P}{2} = 148,800 \text{ km} ,$$

$$e = \frac{A - P}{A + P} = 0.956 ,$$

$$T = \frac{2\pi a^{3/2}}{(GM)^{1/2}} = 6 \text{ days},$$

$$n = \frac{2\pi}{T} = 2.5 \frac{\text{deg}}{\text{hr}} ,$$

$$v_P = \sqrt{\frac{GM}{P}(1 + e)} = 10.9 \frac{\text{km}}{\text{sec}} .$$

If the velocity at perigee is to be used in determining the apogee distance, more significant digits

must be carried. The following formula demonstrates the sensitivity of the apogee distance to small changes in the velocity at perigee:

$$\frac{dA}{dv_P} = v_P \frac{(2a)^2}{GM}$$

If $\Delta v_P = 0.001$ km/sec, then $\Delta A = 2500$ km. The ratio of the velocity at apogee to that at perigee is

$$\frac{v_A}{v_P} = \frac{1 - e}{1 + e} = \frac{P}{A} = 0.0227 .$$

The velocity at perigee is about 10.89 km/sec. At apogee the satellite will be moving 0.25 km/sec, or with an angular motion of

$$\frac{v_A}{A} = 0.17 \frac{\text{deg}}{\text{hr}} .$$

## Time Position Calculations

If the angular distance ($\nu$) of the satellite from perigee measured in the orbital plane is known, the radial distance can be computed from

$$r = \frac{a(1 - e^2)}{1 + e \cos \nu} .$$

The time since last perigee may be related to the radius vector by the equation

$$r = a(1 - e \cos E) ,$$

where $E$ is the eccentric anomaly. The time from the previous perigee passage is

$$t = \frac{1}{n} (E - e \sin E)$$

$$= \frac{T}{2\pi} (E - e \sin E) ,$$

where $E$ is expressed in radians.

Using the IMP numbers obtained above we shall determine the amount of time the satellite will spend beyond the earth's magnetic field, assuming $r$ = 100,000 naut. mi or 185,200 km to be the limit of the earth's magnetic field. This gives

$$\cos E = \frac{1}{e}\left(1 - \frac{r}{a}\right) = \frac{1}{0.956}\left(1 - \frac{185,200}{148,800}\right) = -0.256 .$$

Because of the symmetry of the ellipse, the eccentric anomaly E may be in either the second or third quadrant. The second quadrant value of E is used to determine the time of entry into the region beyond 185,200 km:

$$E_1 = 104.2 \text{ deg} ,$$

$$t_1 = T\frac{1}{2\pi}(E_1 - e \sin E_1)$$

$$= T\frac{1}{2\pi}(1.818 - 0.956)$$

$$= T(0.142) .$$

The time of exit is found from the third quadrant value of E:

$$E_2 = 255.8 \text{ deg} ,$$

$$t_2 = T\frac{1}{2\pi}\left[4.464 - (0.956)(-0.967)\right]$$

$$= T(0.858) .$$

The percent of the orbital period spent beyond the earth's magnetic field is

$$\frac{100}{T}(t_2 - t_1) = 72 \text{ percent} .$$

## Calculations From Injection Conditions

From a complete set of injection parameters, $(r, \phi, \lambda, v, z, \gamma)$, the entire set of elements may be obtained. The inclination is given by

$$\cos i = \cos \phi \sin z .$$

The semimajor axis is

$$a = \frac{r\,GM}{2GM - rv^2} .$$

The right ascension of the ascending node ("node") in degrees is

$$\Omega = \psi + \lambda_{inj} \Delta\lambda - 180 ,$$

where

$$\Delta\lambda = \sin^{-1} (\cot i \tan \phi) \qquad (0 \leq \Delta\lambda < 180 \text{ deg}) .$$

(This implies a launch above the descending node, i.e., a southward direct launch from above the equator.) The signs are explained by Figure 2. The value of $\psi$ may be calculated by finding the H.A. of the First Point of Aries (sidereal time) at midnight of the launch date (Reference 2), adding the universal time hours, and converting to degrees. For Explorer XII $\Delta\lambda$ is 22°34'.

The Greenwich hour angle of the Vernal Equinox moves through 360 deg in just under 1 day. The value of the Greenwich hour angle of the Vernal Equinox at midnight moves through 360 deg in a year. The right ascension of the ascending node varies in the same manner since it is linearly related to $\psi$.

If the satellite is injected into orbit at perigee (elevation angle = 0, r = p), the argument of perigee is

$$\sin \omega = \frac{\sin \phi}{\sin i} \qquad (i \neq 0) ,$$

and the eccentricity is

$$e = 1 - \frac{P}{a}$$

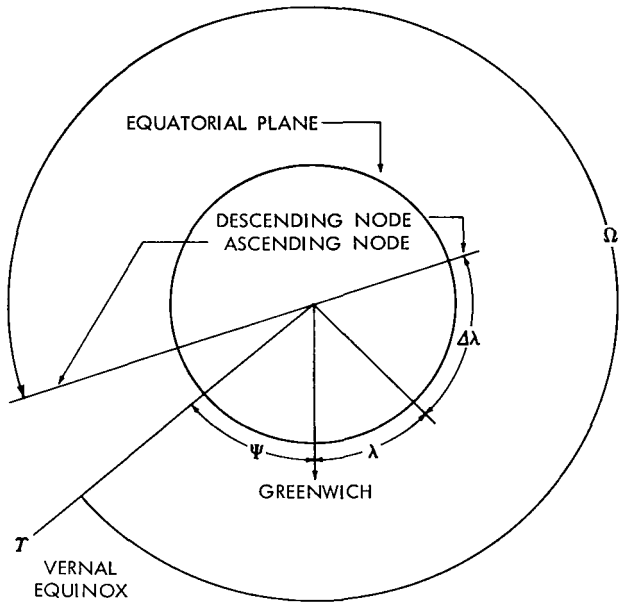


Figure 2—Transformation from longitude of injection to right ascension of ascending node.

## METHODS OF ORBIT COMPUTATION

The differential equations of motion of a satellite acted on by an inverse-square force field (i.e., a spherical earth) have 6 constants of integration which are usually expressed by the orbital elements. For 6 given initial coordinates, the position and velocity of the satellite may be obtained at any future time from the constants of integration. Closed form solutions have not been obtained for satellites affected by more than one force. Future positions of bodies acted on by more than one force are obtained by numerical integration (termed "special perturbation methods" because only one trajectory may be studied at a time) or by the development of approximate theories which assume solutions in the form of infinite series ("general perturbations"). The former method

(combined with a high speed computer) is useful for artificial satellites because the construction of a theory is laborious and because the accuracy and applicability of a theory usually can be determined only by comparison with observation or with numerical integration. Computer programs based on numerical integration can be constructed to be applicable to a wide variety of problems.

The straightforward method of computing the trajectory of a particle acted on by an arbitrary number of forces is to numerically integrate the equations of motion in rectangular coordinates (Cowell's Method). This often suffers from loss of accuracy due to round off or truncation. Two numerical integration programs based on the transformation and modification of the differential equations of motion are in current use.

The Interplanetary Trajectory Encke Method Program (Reference 3) is based on a modified Encke Method. The differential equations of motion of a satellite subject to any number of arbitrary forces are transformed by removing the motion due to the central force and integrating the differential accelerations from the two-body solution due to the perturbations. The reference ellipse is rectified automatically when the perturbed coordinates become appreciable compared with the two-body coordinates. These gravitational forces are included in the program: that of the earth with second, third, fourth, and longitudinal harmonics; that of the moon with triaxial effects; that of the sun; and those for the planets Jupiter, Mars, and Venus. Also included are the atmospheric drag of the earth's atmosphere and radiation pressure. The positions of the planets, moon, and sun are obtained from the interpolation of tables supplied by the Naval Observatory. The planetary tables for 10 years have been stored on an auxiliary tape.

The output quantities are in several coordinate systems. The basic results of computation are the position and velocity vectors in cartesian coordinates in the "inertial" coordinate system centered on the primary force. These coordinates are transformed into osculating elements. Polar coordinates, radar coordinates for up to 72 arbitrary stations, the magnetic "B,L" coordinates, and cartesian coordinates with respect to several celestial bodies are included in the possible output.

Subroutines are utilized to calculate the time behavior of the spin-axis sun angle, apogee-sun angle, and other quantities pertaining to experiment performance.

The Interplanetary Trajectory Encke Method (ITEM) Program is applicable to orbital calculations for close earth satellites, cislunar and translunar satellites, and interplanetary probes. The machine time to compute a high eccentricity orbit about the earth for a year is about 1/2 hr. As applied to high eccentricity orbits, ITEM is used to ascertain which fast-running programs have sufficient accuracy for stability computations and to provide computations when sufficient accuracy is not otherwise obtainable, particularly for the behavior of early orbits and for quantities which depend upon the instantaneous position of the satellite.

The Halphen Program developed by Peter Musen and Arthur Smith (Reference 4) provides "average" orbital changes with much less machine time—1 min per year. The theory of the lunar disturbing action on an earth satellite is based on Halphen's form of the Gaussian method for

obtaining a numerical coefficient of the long period terms. In this method the disturbing force and the momentum are averaged numerically over the mean anomaly of the moon and then over the mean anomaly of the satellite. The numbers obtained give numerical coefficients for the differential equations of the changes in orbital elements.

The disturbing force of the sun is computed with Legendre polymonials. The differential equations are numerically integrated, with integration intervals of 10 days. Machine time required for 1 year's orbit computation is less than 1 min. This method computes average values of changes in the orbital elements. Those variations which are a function of the satellite's or the moon's position are omitted in order that the general trend of an orbit may be established in a minimum of machine time. The method is used to study the long period variations of orbits totally inside the orbit of the disturbing body.

The Lifetime 14 Program, developed by R. Bryant and R. Devaney of Goddard Space Flight Center, is employed to study the effect of atmospheric drag on near-earth satellites. This program numerically averages the drag force over 1 orbit. The atmosphere is based on the Harris-Priester atmosphere (Reference 5) and is time dependent. Gravitational forces are included as Legendre polynomials. The program is useful for high eccentricity orbits to determine at what perigee height the drag force becomes appreciable. Three minutes of machine time will compute the orbit for a year if an atmospheric model that is constant in time is employed.

The orbital changes obtained from the different programs for equivalent starting conditions were compared to establish their relative accuracy. Figure 3 is a comparison of perigee heights for a nominal S-3 orbit. The smooth line is constructed from points computed by Halphen's method. The circles are perigee points obtained by ITEM. They follow the smooth curve closely. The irregularity of the deviation from the smooth curve occurs because ITEM computes the variations due to the position of the moon. Figure 4 compares the influence of gravitational perturbations

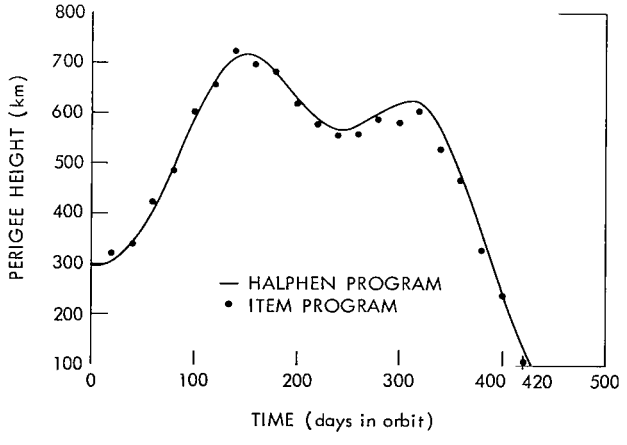


Figure 3—Program comparison of perigee heights for a nominal S-3 orbit with an assumed launch date of August 7, 1962, $\Omega_0 = 201$ deg.

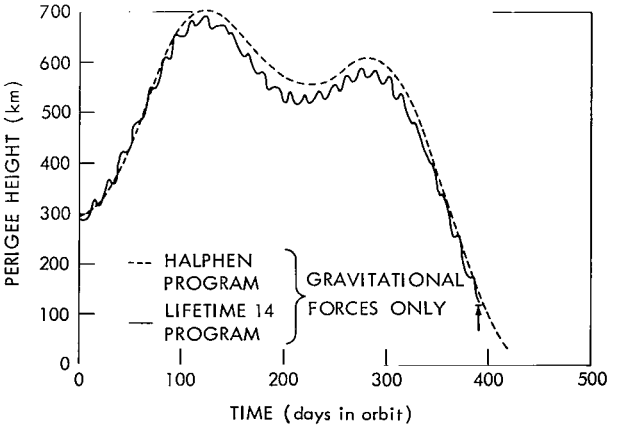


Figure 4—Program comparison of perigee heights for a nominal S-3 orbit with an assumed launch date of September 6, 1962, $\Omega = 206$ deg.

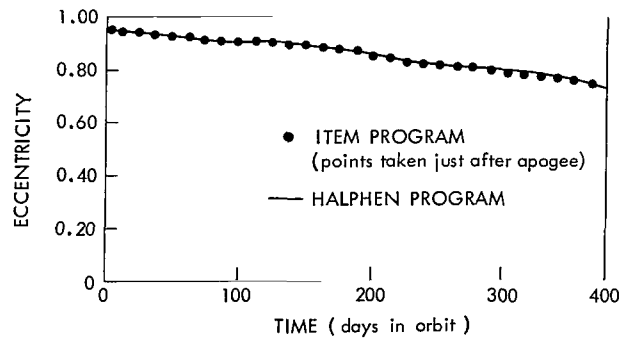


Figure 5—Eccentricity vs. time for an IMP orbit.

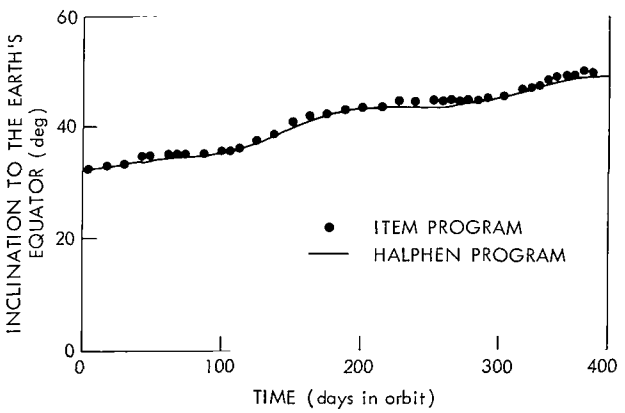


Figure 6—Inclination vs. time for an IMP orbit.

on perigee height as obtained from the Lifetime 14 and Halphen Programs. The oscillations in the Lifetime 14 curve are due to the short period Moon effect. The curves agree well, indicating that this program will calculate gravitational perturbations on S-3 orbits accurately.

The IMP orbit is a stringent test of a partially analytic method because of the large semimajor axis (1/3 lunar distance) and the large eccentricity (0.95). Figures 5 and 6 compare the history of the eccentricity and inclination for 1 year as obtained by ITEM and the Halphen Program. Although the inclination has changed from 33 to 54 deg by the end of the year, the results of the two programs do not diverge.

Deviations between program results have two sources: (1) short period oscillations computed by ITEM which are smoothed out by the Halphen Program; (2) the difficulty of obtaining equivalent starting conditions; i.e., of determining the constants of integration of the theories. ITEM is started from injection conditions at perigee. Orbital elements are selected from the trajectory computed by ITEM to initiate the Halphen Program. In order to reduce the osculating effects of the oblateness (see the next section), the elements are selected at some distance from the earth.

## PERTURBATIONS

The field of celestial mechanics developed from observations of planetary motion. Perturbation theories have been developed extensively for the planets, because of the accuracy and quantity of observations. Changes in the orbital elements for planets are slow and the orbital periods are long, compared with human life span. Artificial satellites have shown novel perturbation effects, and present opportunities for future mathematical developments.

The perturbations on artificial satellite orbits considered originally were those due to the atmosphere and the oblateness (equatorial bulge) of the earth. The value of the third harmonic ("pearshape") of the earth was obtained from Vanguard data by O'Keefe, Eckels, and Squires

(Reference 6). Many have calculated the perturbing effects of radiation pressure on the balloon satellite Echo I (1960 1). The effect of the moon and sun on the eccentricity of the orbit of Explorer VI (1959 1) was announced by Kozai (Reference 7). It was suggested by Musen, Bailie, and Upton (Reference 8) that the effect on the eccentricity, i.e., on perigee, could adversely affect the lifetime of a satellite. Preliminary studies for the IMP showed large and rapid changes of inclination as well as eccentricity (Reference 9); similar effects have been found by Hamid on the high eccentricity orbits of asteroids, which are perturbed by Jupiter*.

Practical applications of lunar-solar perturbations were initiated by Bailie, who showed that varying the hour of the launch of EGO would change the lifetime of the satellite from between a few orbits to at least a year. Explorer XII was launched at a time which would insure a lifetime of a year.

## Definitions

For the purpose of discussion, three arbitrary definitions will be made. (These are analogous to terms referring to analytic theories, but are derived here from the examination of numerical results.) "Osculating elements" denotes the elements obtained from a conversion of the instantaneous position and velocity coordinates. They are considered to be approximately averaged after 1 period. "Short period effect" will be applied to oscillations in the elements which are functions of the instantaneous position of the moon or sun. In particular, there is a very pronounced and apparently universal oscillation with periods of 1/2 the period of revolution of the disturbing body (Reference 10). "Long period effects" will describe changes in the elements which occur over many orbits of the satellite and the disturbing body. They depend on the relative orientations of the orbits rather than the relative positions.

Short period and osculating effects are considered to cause small, temporary departures from the long period effect. It may be seen that these effects are imperceptible on a graph of a complete long period cycle.

Two types of perturbations are distinguished here, "direct" and "indirect" (or "coupled"). The direct effect is the variation of the elements that is computed by assuming a single disturbing force. Indirect effects are variations in the elements which occur when several perturbing forces are present and do not occur when any one force is considered alone. (Coupling will be considered here only between forces; the discussion will implicitly treat "cross-actions" between the elements, but not explicitly.) The magnitude of the element variations due to coupled forces may be large enough to determine the lifetime of the satellite. For example, the oblateness of the earth will cause the orientation of the orbit to rotate in space. The strength of the changes in the inclination and eccentricity depends upon the orientation of the satellite orbit with respect to the plane of the moon or sun. Therefore, although the oblateness does not affect the eccentricity directly, it causes

* Public comment at the American Astronomical Society Conference, Cambridge, Massachusetts, 1962.

the perturbation of the eccentricity by the moon and the sun to be different. This effect is very strong on S-3 orbits, since they are close enough to the earth to have motions of $\Omega$ and $\omega$ of 0.1 deg/day. The effect of atmospheric drag can be studied essentially independently, since the perigee height of a high eccentricity orbit moves rapidly from regions where the drag force is negligible to heights where it is magnitudes larger than all other forces.

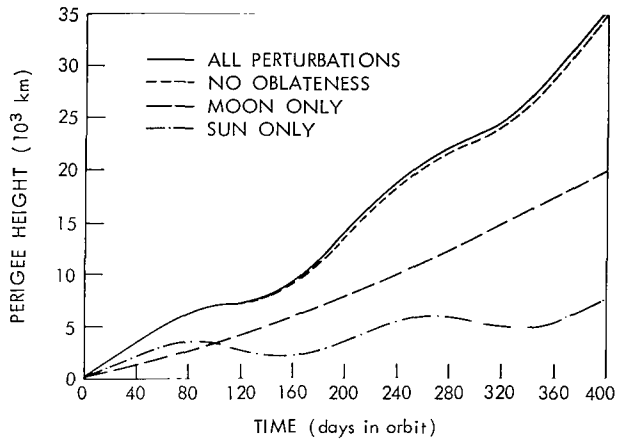


Figure 7—Effect of perturbations on perigee height for an IMP orbit (Halphen Program).

Gravitational perturbations will be considered in several ways. First an IMP orbit will be described as if only the moon perturbed it, then as if only the sun perturbed it, and then with the sun and moon combined to perturb it. The effect of the oblateness on this orbit is relatively small during a year (Figure 7), since the orbit "sees" the earth for the most part as a sphere. An S-3 orbit will be considered with all these gravitational perturbations included, since the *coupling* of lunar and solar perturbations with the oblateness perturbations determines the lifetime.

## Disturbance by the Moon Only

The idealization that only lunar effects are disturbing the orbit is made for illustrative purposes. Halphen's method is used to numerically integrate the long period perturbations. The curves in Figure 8, showing typical long period behavior, were computed from the starting conditions

$a = 22.8$ earth radii, $e = 0.95$,

$i = 33$ deg, $\omega = 270$ deg, and $\Omega = 270$ deg .

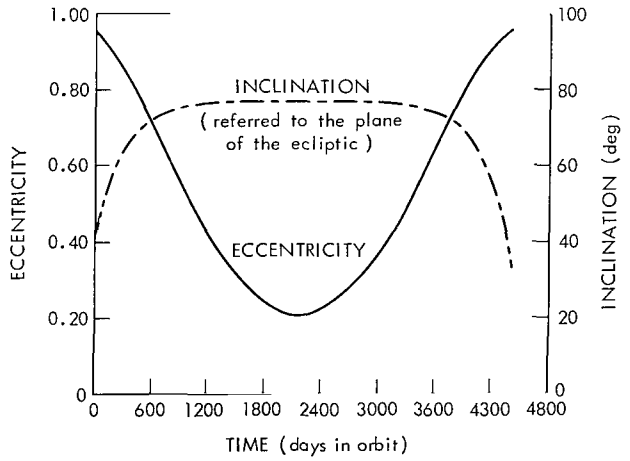


Figure 8—Eccentricity and inclination vs. time for an IMP orbit of 10 years (Halphen Program).

The variation in the eccentricity has a period of about 12 years. (Computation ceased automatically when the perigee reached the earth's surface.) The eccentricity curve is like a sine wave, with a minimum of 0.2 and a maximum near 1. (An eccentricity of 1 implies a degenerate ellipse and not a parabola, unless there is also escape energy.) The inclination with respect to the disturbing plane moves up rapidly until it reaches a plateau at 81.9 deg. It does not vary appreciably while the eccentricity goes to a minimum but it decreases again when the eccentricity returns to high values.

The period of the long period perturbations on the elements is unexplained at present. A qualitative explanation of the shape of the eccentricity and inclination curves may be derived from the integral of the energy of the restricted three-body theory. The integral, obtained by Jacobi (Reference 11), provides the only known constant of this problem:

$$\frac{1}{2} v^2 - n' (x\dot{y} - y\dot{x}) = \frac{GM}{|r_{es}|} + \frac{GM_m}{|r_m|} - C ,$$

where $x$, $y$, $\dot{x}$, $\dot{y}$, and $v$ are cartesian coordinates measured from the center of the earth in the (nonrotating) plane of the moon's orbit, $r_{es}$ and $r_{sm}$ are the distance from the satellite to the earth and to the moon, $n'$ is the mean motion of the moon, and $C$ is the constant of energy obtained from the integration. Under the assumption that the cartesian coordinates can be expressed as two-body elements and that the satellite does not come too near either body, the formula above is converted into Tisserand's criterion for the identification of comets:

$$\frac{1}{2a} + \left[\frac{a(1 - e^2)}{a'^3}\right]^{\frac{1}{2}} \cos i = \text{constant}$$

Assuming that the semimajor axis is constant (which is reasonable for orbits inside that of the disturbing body) gives

$$\sqrt{1 - e^2} \cos i = J_r ,$$

where $J_r$ is approximately constant.

The expression $\sqrt{1 - e^2} \cos i$ is the component of angular momentum perpendicular to the plane of the disturbing body expressed in two-body terms. For objects with circular orbits oriented in the plane of the disturbing body $J_r = 1$. It is not possible, in this case, to change $e$ or $i$ without changing the "constant" $J_r$; hence, by this reasoning circular orbits with zero inclination are stable. If $e$ is near 1 or $i$ is near 90 deg, then $J_r$ is small. Large changes in one element may be compensated by changes in the other. In a rule-of-thumb sense, it may be said that a decrease in eccentricity will be correlated with an increase in inclination. The plateau in the inclination is explained as follows: $\sqrt{1 - e^2}$ does not change much with respect to changes in $e$ when $e$ is small.

Kozai (Reference 12) has studied by semi-analytic methods the general characteristics of long period perturbations. His results indicate that the eccentricity will increase while the argument of perigee is in the first or third quadrant with *respect to the orbital plane of the disturbing body* and decrease while the argument of perigee is in the second or fourth quadrants. Therefore, the early behavior of perigee height is controlled by the orientation of the satellite orbit.

The elements calculated by the Halphen method are average values, excluding fluctuations which depend upon the satellite's and moon's positions. The fluctuations in the elements around the

long period trend are small, but large enough to be significant on the IMP orbit when perigee is very low, i.e. at launch.

## Disturbance by the Moon and Sun

The sun's disturbing force is expanded in Legendre polynomials. Its effect on the orbit is numerically integrated along with the moon's disturbing effect obtained by Halphen's method. Figure 9 compares the effect of the sun alone, the moon alone, and the combination of the two on the eccentricity of the IMP orbit discussed above.

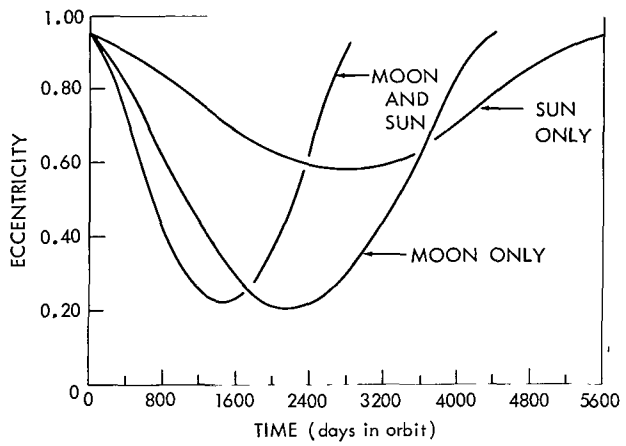


Figure 9—Comparison of perturbations on an IMP orbit for a 10 year period (Halphen's Program).

In Figure 5 the first year of the moon-and-sun calculation is compared with the osculating elements computed by the ITEM Program. The oscillation in the eccentricity curve is due to a short period sinusoidal sun term (imperceptible on the scale of Figure 9) superposed on the long period trend. The period of the term is 1/2 year and the amplitude of this variation in perigee height is 1000-2000 km on the IMP orbit, 100-200 km on the EGO orbit, and 100 km on the S-3 orbit.

## Oblateness

The S-3 orbit is perturbed heavily by the second harmonic of the earth because it frequently passes near the earth. Therefore, this orbit will be used to demonstrate the effect of the oblateness.

The right ascension of the ascending node and the argument of perigee have secular perturbations approximated by

$$\frac{d\Omega}{dt} = -\frac{Jn \cos i}{\left[a\left(1 - e^2\right)\right]^2} ,$$

$$\frac{d\omega}{dt} = \frac{Jn}{\left[a\left(1 - e^2\right)\right]^2}\left(\frac{4 - 5 \sin^2 i}{2}\right),$$

where $J = 1.6208 \times 10^{-3} R_e^2$ and $R_e$ is the radius of the earth (Reference 13). For the nominal S-3 orbit

$$a(1 - e^2) = 12060 \text{ km} ,$$

$$\cos i = \cos 33 \text{ deg} = 0.84 ,$$

$$n = \frac{2\pi}{T} = \frac{2\pi \text{ rad}}{1.25 \text{ day}}$$

$$\dot{\Omega} = -1.62 \times 10^{-3} \left[\frac{6378 \text{ km}}{12060 \text{ km}}\right]^2 \frac{2\pi}{1.25} (0.84)$$

$$= -1.91 \times 10^{-3} \frac{\text{rad}}{\text{day}} = -0.11 \frac{\text{deg}}{\text{day}} ,$$

$$\dot{\omega} = -\dot{\Omega} \frac{4 - 5 \sin^2 i}{2 \cos i} = +0.16 \frac{\text{deg}}{\text{day}} .$$

The oblateness has no appreciable secular effect on the other orbital elements in a direct sense (Reference 14).

## Combination of Gravitational Forces

Coupling effects of the oblateness and the lunar solar perturbations may appreciably change the lifetime of a satellite. The perturbing force of the oblateness changes the orientation of an orbit with respect to the disturbing planes of the moon and sun, thereby modifying the phase of the perturbation on the eccentricity.

Typical perigee height curves are presented in Figure 10 for S-3. They were calculated by an analytic method which considers only the perturbations on the eccentricity by the moon and sun, and on the right ascension of the ascending node and the argument of perigee by the oblateness. This method, when checked by numerical integration, is found to be sufficiently accurate for a year's computation of the perigee height of S-3.

Plots of the osculating elements for the first Explorer XII orbit demonstrate the complexity of perturbations acting in conjunction (Figures 11-16). Sharp spikes occur in the curves at perigee and are due to the earth's oblateness. The spikes in the semimajor axis and eccentricity are averaged out after the perigee pass. Drops or rises in $\Omega$ and $\omega$ are secular and equivalent to the values of the formulas above. The values of the elements, as determined from the coordinates at perigee, are not representative. For instance, the period computed at perigee is 26.40 hr., whereas the actual time between perigee passage is 26.20 hr. These curves were calculated by ITEM with all major gravitational perturbations included. The downward drift in the eccentricity is due to the sun and moon.

## Atmosphere

The atmosphere's drag will directly affect the orbital elements $a, e$ and $\omega$ (Reference 14). Indirectly it will affect the rates of rotation of the node, argument of perigee, and inclination if the

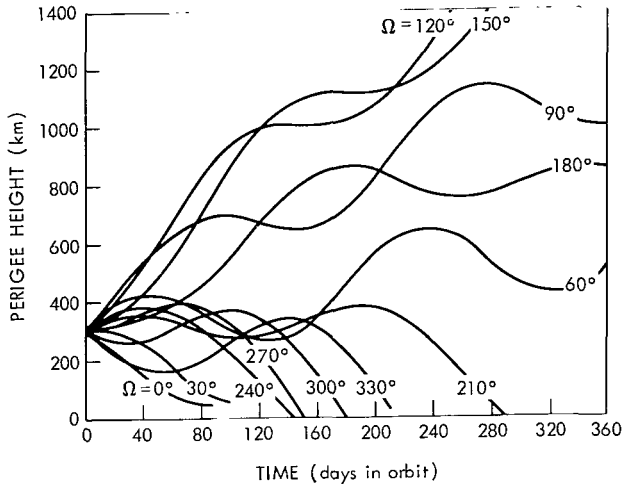


Figure 10–Solar-lunar perturbation effects on perigee height for an S-3 orbit.

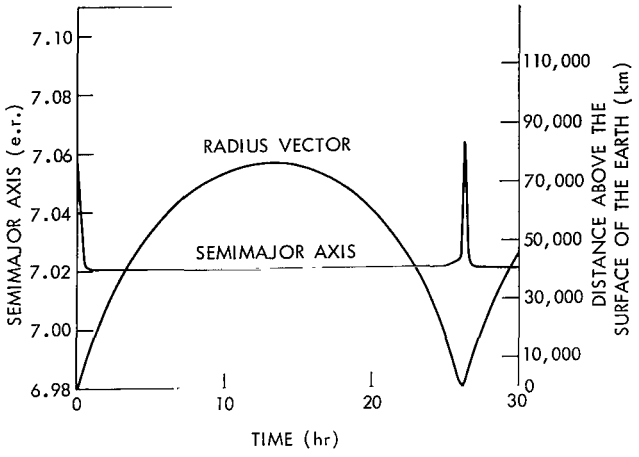


Figure 11–Semimajor axis and radius vector vs. time for the first orbit of Explorer XII.

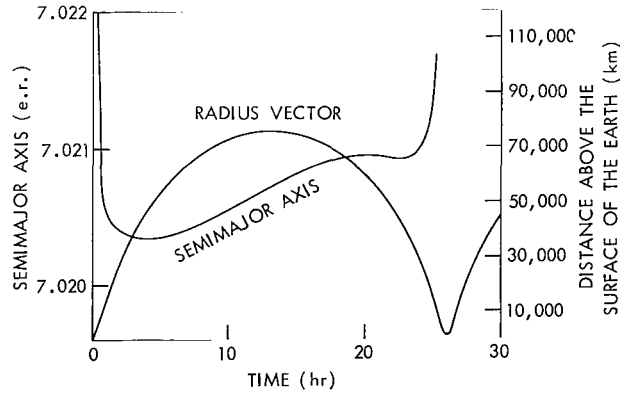


Figure 12–Semimajor axis (expanded scale) and radius vector vs. time for the first orbit of Explorer XII.

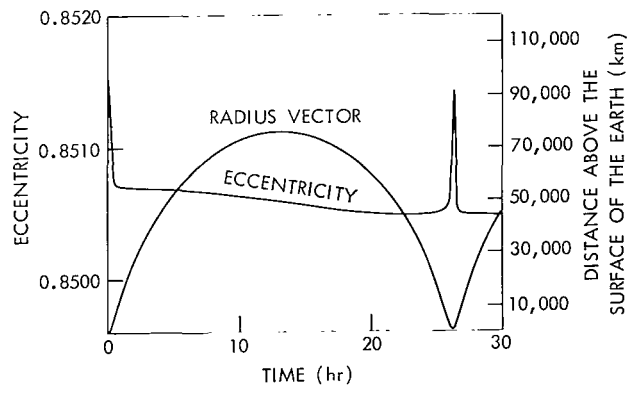


Figure 13–Eccentricity and radius vector vs. time for the first orbit of Explorer XII.

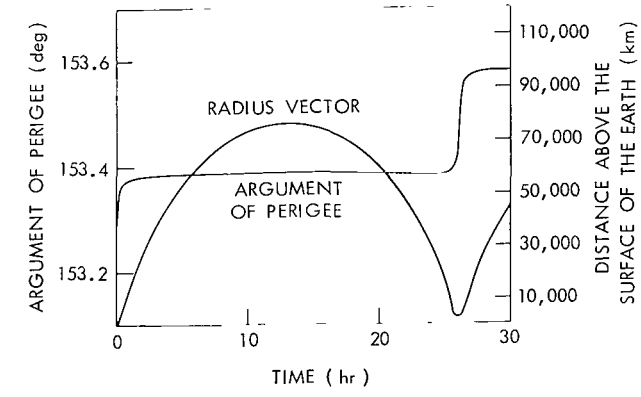


Figure 14–Argument of perigee and radius vector vs. time for the first orbit of Explorer XII.

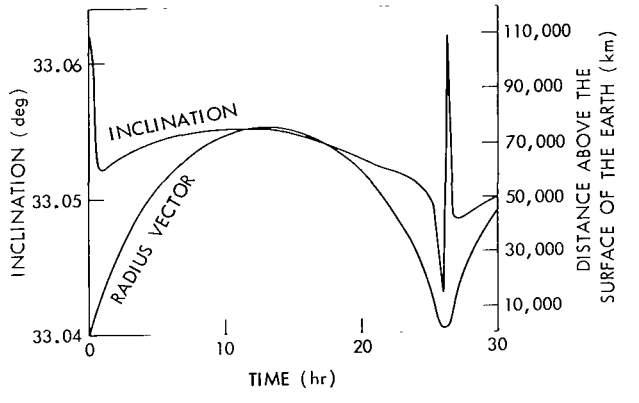


Figure 15–Inclination and radius vector vs. time for the first orbit of Explorer XII.

changes in a and e are large enough to change the magnitude of the solar and lunar or oblateness perturbations on the other elements. In a high eccentricity orbit these indirect or coupled effects are negligible because of the very sharp line of demarcation above which perigee is at a height where the atmosphere has a negligible effect on the history of the orbit and below which the atmospheric perturbation dominates all others, changing the orbit severely during every perigee pass and killing it within a few orbits.

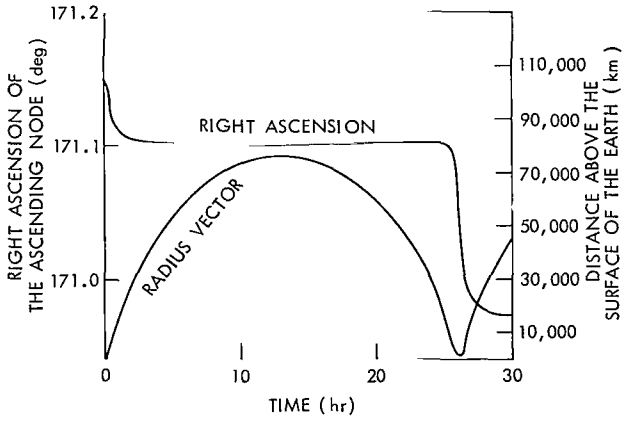


Figure 16—Right ascension of the ascending node and radius vector vs. time for the first orbit of Explorer XII.

The effect of atmospheric drag has been studied in detail for the S-3A orbit with ITEM and Lifetime 14. A drag coefficient of 0.23163 $cm^2/gm$ (maximum cross-section) was assumed for the satellite. The atmospheres assumed were: (1) model 7 in Report 25 of the Smithsonian Astrophysical Observatory (Reference 15), fitted to an Air Research and Development Command (ARDC) model atmosphere of 1956 (Reference 16) at the low altitude in the ITEM Program; (2) the atmosphere developed by Priester and Harris in the Lifetime 14 Program.

Above 300 km the atmosphere has a negligible effect on the orbit. The total reduction in the semimajor axis after 360 days in orbit is 15 km in the case illustrated in Figure 17. This is an average reduction of 0.05 km ($10^{-4}$ percent) on each perigee pass. The reduction in the semimajor axis is plotted on semilog paper as a function of perigee height for perigees below 350 km in Figure 18. Until about 120 km, the percent reduction in the semimajor axis is small. Changes of this magnitude in the semimajor axis (and the eccentricity which is also slight because of drag) do not change the rates of rotation of the node and argument of perigee. For example, one S-3 orbit in which atmospheric drag had reduced the semimajor axis by 3000 km had differences in the angular elements of the order of 0.1 deg, when compared with numerical results from the same starting conditions with atmospheric drag omitted.

A couple of points at 150 km computed by ITEM compare well with those computed at 150 km by Lifetime 14. Points at 110 km do not agree as well because: (1) at this height the atmospheric density changes rapidly, amplifying small computational differences in perigee height; (2) the integration interval used in Lifetime 14 is too large for the rapid orbital changes.

When lunar-solar perturbations have driven perigee to 120 km or less, drag will rapidly kill the orbit. A sample case calculated by ITEM is tabulated in Table 1 to show the final orbits.

## Comparison of Data With Theory for Perigee Rise

Figure 19 compares the theoretical perigee rise of the Explorer XII orbit with data obtained during the first 3 months after launch, while the transmitter was functioning. The smooth curve

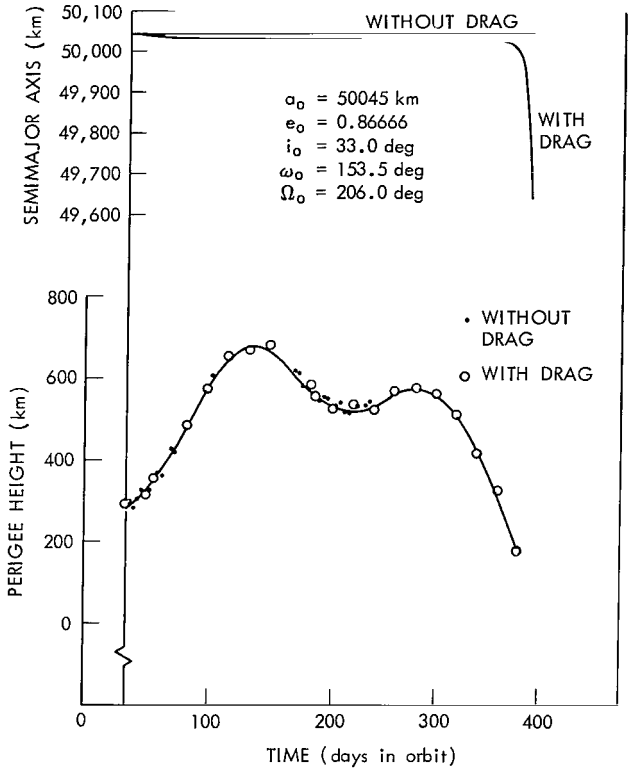


Figure 17—Effect of drag on an S-3 orbit for an assumed launch date of August 7, 1962 (Lifetime 14 Program).

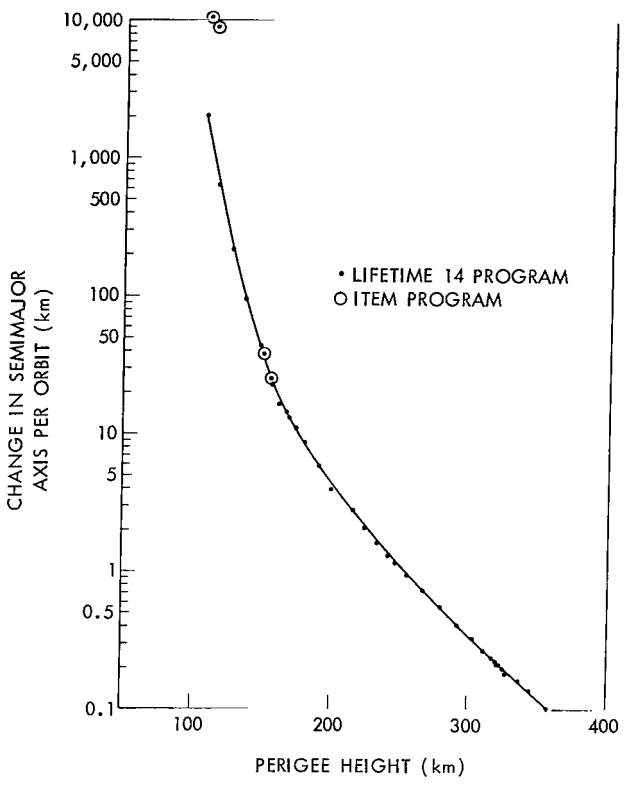


Figure 18—The reduction of the semimajor axis per perigee pass vs. the perigee height, for the case illustrated in Figure 17.

Table 1

Final Orbits

| Semimajor Axis (earth radii) | Equivalent Period (hr) |
|---|---|
| 7.2 | 27.2 |
| 5.6 | 18.8 |
| 4.0 | 11.3 |
| 3.0 | 7.2 |
| 2.4 | 5.1 |
| 1.9 | 3.7 |
| 1.6 | 2.9 |
| 1.4 | 2.3 |
| 1.2 | 1.8 |

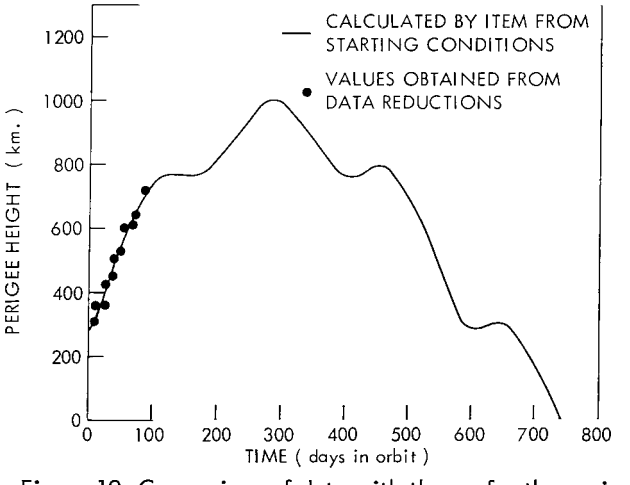


Figure 19—Comparison of data with theory for the perigee height of Explorer XII.

in Figure 19 is the result of computation by ITEM with initial conditions obtained from data reduction and no subsequent differential correction. Each point is observed data smoothed for a week. A consistent trend is seen for the 3 months, the perigee rising from 300 to 700 km. Extrapolation of this curve predicts a maximum perigee height of 1000-1100 km. The orbit must have been terminated by the lowering of perigee into dense regions of the atmosphere in August 1963.

## AUXILIARY CALCULATIONS

We wish to calculate parameters which affect the experiment objectives and spacecraft performance. These quantities depend upon the particular satellite; a few are discussed in this section. Stress is placed on the geometric point of view.

### Shadow

The time a satellite spends in the shadow depends on the alignment of the orbit with respect to the sun. The longest time occurs when the apogee is in the shadow and directly on the earth-sun-line. For a cylindrical shadow, the radius vector at the intersection of the shadow and the ellipse, when the line of apsides is coincident with the earth-sun-line is

$$r = a \pm e\sqrt{a^2 \frac{(1 - e^2) - R_e^2}{1 - e^2}}$$

where the positive root holds when apogee is in the shadow and the negative root when perigee is in the shadow. (If $R_e$ is negligible compared with $a$, the formula reduces to the calculation for apogee and perigee.) If $e = 0.8666$ and $a = 7.8$ earth radii (e.r.), then $r = 1.3$ and 14.3 e.r. If perigee is centered in the shadow, the eccentric anomaly at exit from the shadow is 15.9 deg and the exit time is 0.196 hr. ($T = 30.9$ hr) after perigee passage. From the symmetry of the equations, it is seen that the same amount of time is spent in shadow from entry to perigee passage. So the total time in shadow for the case when perigee is in the center of the shadow cylinder is 0.392 hr. or 24 min. For apogee centered in the shadow, the angle of entry is 164.9 deg; the time spent between entry into shadow and apogee is

$$\frac{T}{2\pi}\left[\pi - (E - e \sin E)\right] = 2.5 \text{ hr}$$

and the total time in shadow is 5 hr.

For the case where the center of the shadow coincides with the line satisfying the condition $\nu = 90$ deg ($\nu$ is the true anomaly), the radius vector on entering the shadow is

$$r_{in} = a(1 - e^2) - eR_e$$

and on leaving the shadow it is

$$r_{out} = a(1 - e^2) + eR_e$$

For the values of $a$ and $e$ used above $r_{in} = 1.084$ and $r_{out} = 2.816$. The total time in shadow, that is, the difference between the times obtained from $r_{in}$ and $r_{out}$, is 0.698 hr.

Shadowing will occur twice a year, while the sun is passing one of the nodes formed by the intersection of the orbit and ecliptic planes. If the node is near the line $\nu$ = 90 deg, the duration of shadow during each orbit will be the same at both times of year; otherwise, periods of brief shadow durations will occur when perigee is in the shadow, 1/2 year later each orbit will have a period of lengthy shadow duration when apogee is in the shadow.

Two methods are available for computing the shadow time of any alignment of the orbit. ITEM has a Shadow Subroutine. It compares the coordinates of the satellite with those of the sun at each integration interval to determine whether the satellite is in the sunlight, the penumbra, or the umbra. The time in each region is accumulated and printed out when the satellite enters another region. This provides accuracy at the expense of machine time. For the project planning involved here, an analytic shadow program has been incorporated into the Halphen Program. Accurate orbit elements during the lifetime of the orbit are provided by the Halphen Program. The intersection of the elliptical orbit with a cylindrical shadow is expressed as a quartic, which is solved by numerical iteration.

The accuracy of the two methods in computing the shadow for a year's orbit depends upon the accuracy of the base program (see the earlier discussion on "Methods of Orbit Computation"). ITEM is more accurate over one orbital period because it calculates the instantaneous position rather than assuming an average set of elements for the orbit and a fixed sun and because it allows for the refraction of the penumbra and umbra rather than assuming a cylindrical shadow.

## Spin-Axis Sun Angle

Another calculation to be made is the angle between the satellite's axis of revolution and the line from the satellite to the sun. Various terms are, or have been used to denote this angle, including "optical aspect angle," "solar aspect," and "spin-axis sun angle."

It is assumed in the following that the manner in which the satellite is spun up at injection results in the alignment of the spin axis in the direction of the injection velocity vector. It is also assumed that external torques are negligible and that no internal drives are present.

Geometrically, the behavior of the spin-axis sun angle ($\alpha$) as a function of time may be described as follows. The spin axis is pointed at one spot on the celestial sphere where, under the foregoing assumptions, it remains fixed once the satellite has been launched. It intercepts the celestial sphere at a latitude determined by the direction of the injection velocity vector. The earth's rotation provides every longitude once every 24 hr. The arc $\beta$ between the ecliptic and the point P (Figure 20) where the spin axis intercepts the celestial sphere is the minimum spin-axis sun angle during a year, occurring when the sun is at A ; 180°- $\beta$ is the maximum, occurring 1/2 year later. In the particular case when $\beta$ = zero, $\alpha$ will zigzag between 0 and 180 deg; when $\beta$ = 90 deg, $\alpha$ will always equal 90 deg. Other cases will oscillate between the maximum and minimum $\alpha$ in a "squashed" sine wave (Figure 21).

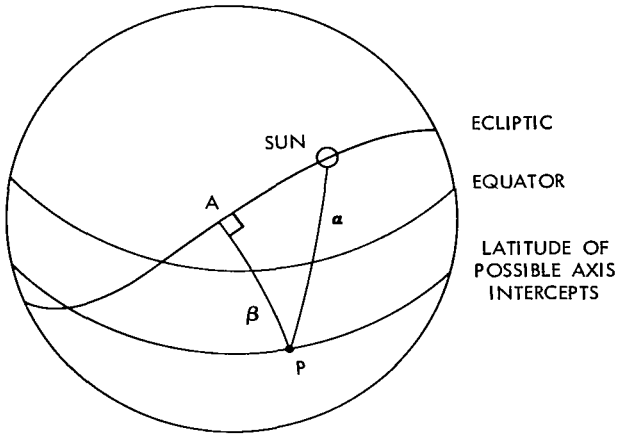


Figure 20—Geometry of the spin axis and ecliptic.

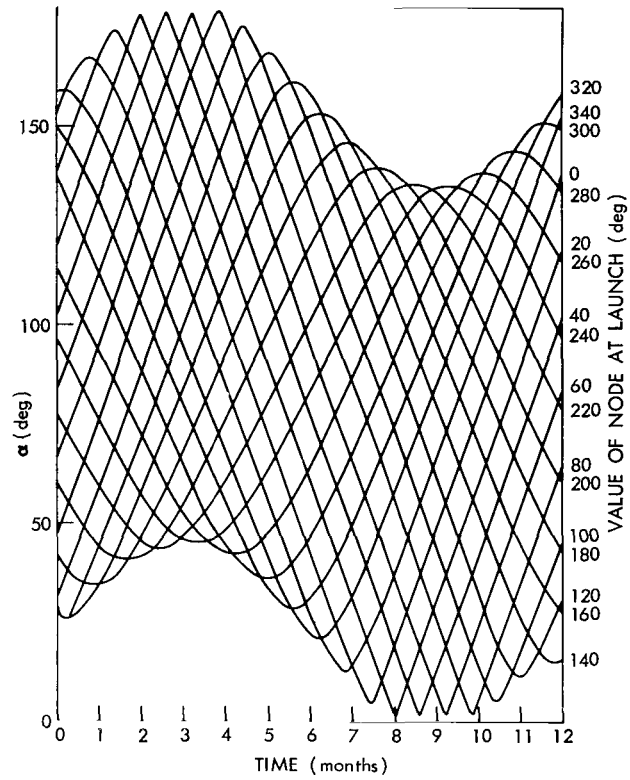


Figure 21—Spin-axis sun angle behavior.

The foregoing paragraph applies to the behavior of the angle between any point fixed on the celestial sphere and a point moving in an arc around the celestial sphere. For example, the same type of relationship will hold for the angle between the apogee and the sun as long as the perturbations on the line of apsides may be neglected.

Mathematically, it is convenient to calculate $\alpha$ by taking the dot product of the initial velocity vector and the vector in the direction of the sun. The former may be obtained by rotating the injection velocity vector from earth-referenced space into inertial space. Or they may be obtained by converting the initial orbital elements into an initial velocity vector; this method is useful because the value of the node assigns a position in latitude on the celestial sphere, independent of the launch day. The sun's coordinates may be obtained within 2 deg by assuming that the sun moves along the ecliptic at a constant rate, and converting its position into cartesian coordinates. This method gives the maximum and minimum spin-axis sun angles by calculating the sun's position at sufficiently close intervals. Its advantages are that machine computation is rapid and use of the node as a parameter allows for a complete analysis with relatively few calculations.

Figure 21 shows the behavior of the spin-axis sun angle for a launch on Jan. O.O. If the node is held constant the maximum and minimum will be the same for any other launch day. The initial phase is obtained by reading from the launch day on the abscissa. For example, if launch were in the fourth month with a $\Omega_0$ = 260 deg, then the initial angle would be $\alpha_0$ = 42 deg; for $\Omega_0$ = 340 deg, $\alpha_0$ = 85 deg; and for $\Omega_0$ = 100 deg, $\alpha_0$ = 166 deg.

An option is available for the ITEM Program which also computes this angle as well as the angle between the spin axis and the normal to the ecliptic. This latter angle provides immediately the maximum and minimum spin-axis sun angles.

## PRACTICAL APPLICATIONS

Specific problems of prelaunch analysis may involve any or all of the computations discussed in the previous sections. High eccentricity satellites with a required minimum lifetime always introduce the problem of finding launch times when solar and lunar perturbations will be favorable. Experiment and spacecraft requirements may also indicate definite launch times. The specific problems discussed in this section are:

1. The construction of a launch window map. The preliminary version of the IMP map is used as an example. A detailed map for EGO is given in Reference 17.
2. The effect of uncertainties in injection conditions due to vehicle tolerances on the orbital parameters and subsequent orbital behavior.
3. The feasibility of controlling the initial launch time to guarantee a maximum as well as a minimum lifetime.

### Launch Window Maps

The term "launch window" arose from lunar and interplanetary probes and designates the time when energy requirements are near the minimum necessary for attaining the mission. This time of minimum energy requirements is a necessary condition for launch when vehicle performance is marginal. For the high eccentricity satellites under consideration "launch window" has the sense of a block of time when all constraints will be satisfied.

*Definitions*

A "constraint" is a requirement on the satellite system. A major constraint on high eccentricity satellites is that the orbital lifetime shall have certain minimum duration—usually a year. Technically it is phrased that "perigee height should not be less than a specified number of kilometers during the first year after launch." The criterion that perigee should not be less than the initial value-300 km for S-3—has been used to guarantee that the atmosphere will not affect the lifetime. Figure 18 suggests that the atmosphere will have negligible effects on the S-3 orbit at 250 km. Requirements on the maximum eclipse allowed and on the orientation of satellite axes with respect to the sun arise from thermal requirements. When possible, spacecraft requirements should be kept to a minimum because of the inflexibility of the constraint from lunar-solar perturbations.

The term "behavior curve" describes figures which show the values of a quantity—for instance, perigee height or spin-sun angle—plotted against time in orbit. Figures 21-25 are examples of

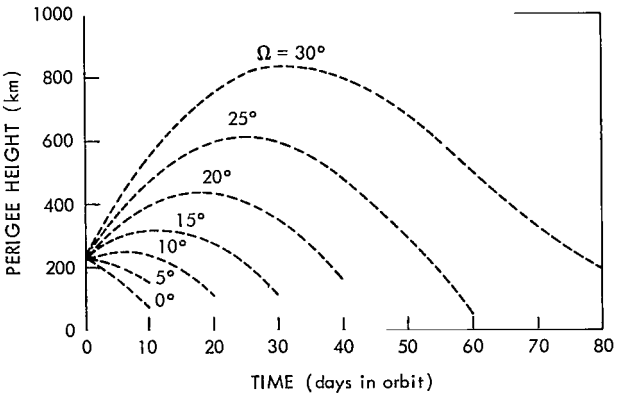


Figure 22—Perigee height vs. time for an IMP orbit with various values of $\Omega_0$ between 0 and 30 deg and an assumed launch date of June 1, 1963.

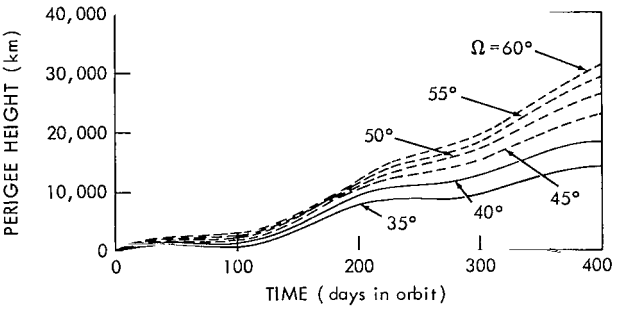


Figure 23—Perigee height vs. time for an IMP with various values of $\Omega_0$ between 35 and 60 deg and an assumed launch date of June 1, 1963.

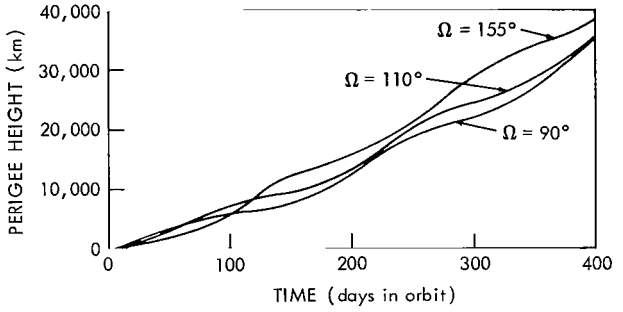


Figure 24—Perigee height vs. time for an IMP orbit with $\Omega_0$ = 90, 110, and 155 deg and an assumed launch date of June 1, 1963.

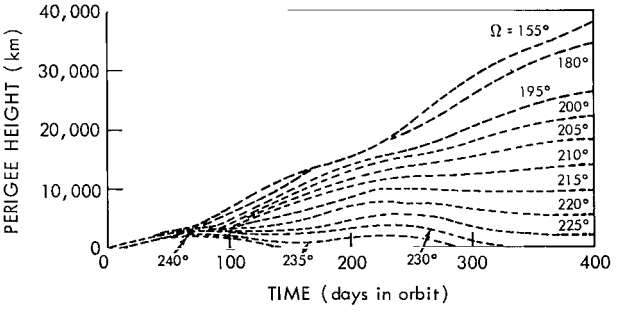


Figure 25—Perigee height vs. time for an IMP orbit with various values of $\Omega_0$ between 155 and 240 deg and an assumed launch date of June 1, 1963.

behavior curves. "Acceptable behavior" occurs when a behavior curve satisfies the constraint at all times during the desired lifetime.

A "launch window" can be defined as a set of hours during the day when all behavior curves are acceptable; that is, if the satellite is launched during the launch window all constraints will be satisfied for a year. The "opening of the launch window" is the earliest acceptable time and the "closing" is the last suitable hour on that day.

A "launch window map" is a complete summary of all the launch windows for the range of time in which launch is scheduled. In advanced planning, it is desirable to construct a launch window for an entire year to show if there are months when the launch window is not open to all.

*Procedure*

In general, the only way to determine a set of launch times when the behavior of a quantity will be acceptable is to select a launch time, calculate the subsequent behavior according to the

methods described in the previous sections, and then examine the whole behavior of the quantity. Behavior calculations are made for new launch times selected by adding increments in hours until the first possible launch day has been spanned. Then new launch days are chosen for the launch period and sets of behavior curves calculated for grids of launch hours on these days. The size of the increments depends upon how critically the behavior curves change with respect to a change in launch time. For several reasons it is necessary to have efficient techniques in organizing the results obtained. Launch window maps are calculated well in advance of pinpointing precise launch days, so studies will cover several months or a year. Calculating behavior curves for every possible hour of launch in that interval would consume enormous quantities of machine time and would involve substantial personnel in reducing the calculations to appropriate forms.

*Referencing to Node*

The behavior of quantities which are functions of the orientation of the orbit in space may be correlated with the value of the node. Each node value is available once every 24 hr, all other parameters being held constant.

The maximum and minimum spin sun angle will be constant for a given value of node, independent of the time of year of launch. The behavior of perigee is approximately constant for a given value of node because the long period effects are much stronger than those depending upon the instantaneous position of the sun or moon (unless the satellite's apogee is 1/2 or more of the lunar distance). The node may be converted into injection time by the formula given in the two-body discussion. If one point is determined, other values may be projected by the approximation that, for a constant time of day, the node value increases by 1 deg on the next day, or conversely, for a constant value of the node the time of day decreases by 4 min on the following day. Figure 26 is a chart of the values of node vs. hours for a month in 1962 (S-3 injection conditions).

*Construction of the IMP Launch Window Map*

The satellite IMP is used here to demonstrate the construction of a launch window map. The map is for the period between June 1963 and June 1964. This is a preliminary version which indicates the rough size of the launch window through the year and allows planning for additional constraints.

Estimates of the injection conditions are made on these assumptions:

1. The initial apogee is 150,000 naut. mi. above the surface of the earth, and the intial perigee is 112 naut. mi. above the surface.
2. Injection latitude = 14 deg, longitude = 49 deg, azimuth = 120 deg, and elevation angle = 0.0.

From these, the initial orbital elements for IMP are obtained as given in the two-body section.

The Halphen Program is used to compute the orbital behavior for a year, assuming the IMP initial orbital elements and a launch date of June 1, 1963. Computations were made at 5 deg

increments for $\Omega_0$ between 0 and 360 deg (72 cases). The integration interval used was 10 days. The case was stopped automatically if perigee was less than 200 km; otherwise it stopped after 40 integration intervals. Machine time for the set of 72 cases is 30 min. Cases were considered to be acceptable if perigee remained above 200 km for a year. The node was converted to hours of the day and the first acceptable time and last acceptable time were plotted on the launch window map (Figure 27). Computations were made for the set of cases every 30 days and acceptable times plotted on the map.

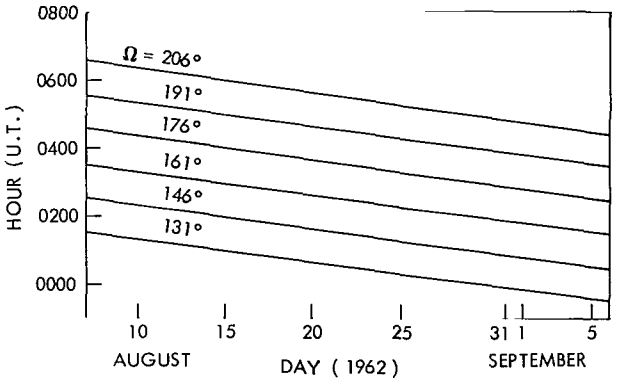


Figure 26–Starting hour vs. launch day for constant nodes (nominal S-3 conditions).

The behavior of cases with initial nodes between 0 and 30 deg is shown in Figure 22. These cases have short lifetimes, no more than 80 days and in some cases as little as 2 or 3 orbits. Strong rising trends of perigee will occur during the first year for starting values of the node between 35 and 200 deg (Figures 23-25, note the changes of the time and kilometer scales). The average rise of perigee in Figure 23 is

$$\frac{36000 \text{ km}}{400 \text{ days}} \times 6 \frac{\text{days}}{\text{orbit}} = 540 \frac{\text{km}}{\text{orbit}} \text{ for } \Omega_0 = 60 \text{ deg}$$

and

$$210 \frac{\text{km}}{\text{orbit}} \text{ for } \Omega_0 = 35 \text{ deg.}$$

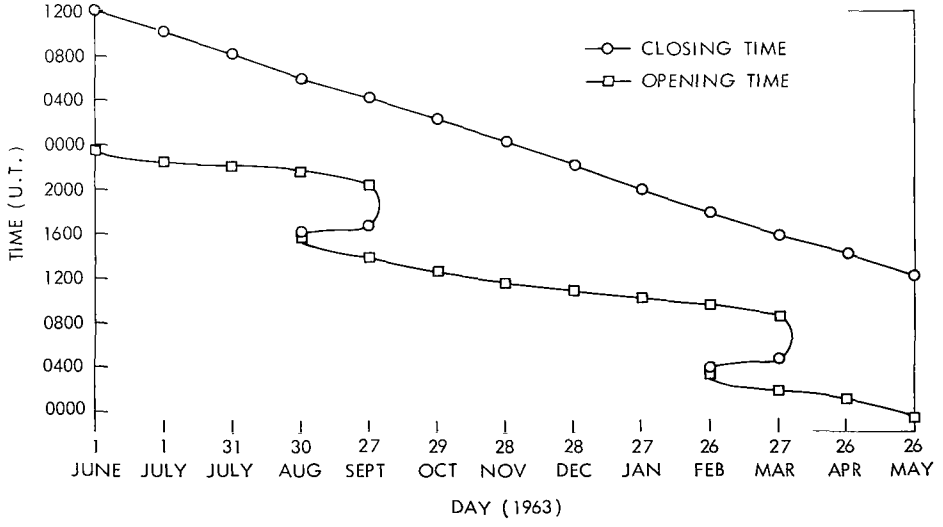


Figure 27–Launch window for IMP, preliminary version considering solar-lunar perturbations.

The dips and rises may be regarded as a sinusoidal curve with a period of about 180 days superposed on an upward trend. The phase of this superposed harmonic depends upon the sun's position (short period sun term), and the initial trend will vary with the time of year of launch for a given value of node. Figure 22 shows only the short period sun term, because of the short time scale. The behavior is plotted for $\Omega_0$ = 90, 110, and 155 deg in Figure 24. Intermediate values of node result in behavior charts so similar that graphing is impractical. Cases of $\Omega_0$ = 155 to 240 deg are plotted in Figure 25. The rate of the perigee rise decreases with increasing node. Perigee for $\Omega_0$ = 215 deg begins to decrease after 240 days. The lifetime is 330 days for $\Omega_0$ = 230 deg, and 150 days for $\Omega_0$ = 240 deg. Higher values of node give even shorter values of lifetime; indeed, in many of these cases the second perigees are substantially below ground, indicating a lifetime of only 1 orbit.

A strong rise in inclination is contingent with the rise in perigee. The value of inclination (with respect to the earth's equator) on the 400th day in orbit is tabulated for various initial values of the node in Table 2. *It should be noted that in many cases the satellite will be moving over high latitudes by the end of the first year in orbit.*

To provide a complete set of possible launch times for the year June 1963 to June 1964, the machine computations of orbital behavior for the 72 cases of node were made for launch dates 30 days apart. The equivalent hour of injection to obtain each value of node on that day was found by the formula given in the two-body section. The first acceptable hour of injection for a given launch day was plotted on a graph with an ordinate of hours of the day and an abscissa of time of the year (Figure 27). (To obtain the launch time, it is necessary to subtract flight time from injection time.) The points determined by computation are indicated by circles if they are the last possible launch time, by squares if they are the earliest possible launch time. For the launch days indicated, orbits have been calculated under the assumption of initial launch times which are 20 min apart (5 deg of node), and these have been examined for a year's lifetime.

Table 2

Inclination after 1 Year for Various Initial Values of the Node

| Initial Node (deg) | Inclination After 1 Year (deg) |
|---|---|
| 40 | 16.3 |
| 50 | 25.9 |
| 60 | 35.8 |
| 70 | 84.1 |
| 80 | 82.0 |
| 90 | 79.2 |
| 100 | 75.9 |
| 110 | 72.6 |
| 120 | 69.3 |
| 130 | 66.2 |
| 140 | 63.3 |
| 150 | 61.5 |
| 160 | 58.7 |
| 170 | 57.1 |
| 180 | 55.0 |
| 190 | 53.2 |
| 200 | 51.1 |
| 210 | 48.0 |
| 220 | 42.3 |

The lower portion of the launch window map contains two areas, 180 days apart, where the window opens for a few hours, closes for a few hours, and reopens for several hours. This "backward S shape" is caused by the short period sun term. Since the amplitude of this effect is on the order of 1000 km, a downward phase of this term superposed on a moderate upward long period trend of perigee will result in a brief net decrease of perigee. If the initial value of perigee is 220, km, a decrease of only 100 km

can prove fatal to the orbit. Orbits in the unacceptable region near this line have very short lifetimes. The upper, nearly straight line is the closing of the launch window. It corresponds to $\Omega_0$ = 220 to 225 deg. As may be seen in Figure 25, these values of node provide lifetimes of a year, the exact lifetime depending slightly on the phase of the short period sun term.

*Lifetime of IMP*

To give an idea of the range of lifetimes, the orbits for sample launch days were computed until a value of perigee less than 200 km occurred. The resulting lifetimes are plotted against $\Omega_0$ in Figure 28 for two starting dates 1/4 year apart. Many of the orbits initiated on different days with the same value of node have the same lifetimes, but an unfavorable phase of the short period sun term changes the 20 year lifetimes to a few orbits. Again, the short period moon term has not been included in this stability study. Qualitatively, though, it may be stated that IMP orbits have lifetimes of a few orbits to a few decades before collision with the earth.

## Accuracy of a Launch Window

The map shown above was used to illustrate technique and is not intended to be a working model. In the actual preparation of a launch window, the following points should be carefully examined:

1. The behavior of perigee as a function of the position of the moon. The Halphen Program does not calculate the short period term. The double amplitude of variations in perigee due to the position of the moon is about 30 km for S-3 and 50-70 km for EGO. It is difficult to estimate the value for the IMP orbit, but fluctuations about the mean trends shown in Figures 22-25 may be hundreds of kilometers. This would not be tolerable during early orbits when perigee is still close to the earth. Since the magnitude of the effect on the IMP orbit is substantial, the first 6 perigee passes *must* be checked by the ITEM Program for *each* launch time under consideration. Because of the larger size of the IMP orbit, compared with S-3 and EGO, and because of the lower height of the initial perigee, many of the orbits found by the Halphen Program to be viable, would in fact be destroyed on the first return to perigee.

2. Vehicle tolerances. Uncertainties in the injection speed can cause differences of months in the lifetimes (Figure 29). The effect on the launch window depends on the orbit and on the size of the tolerances.

3. Experiment constraints. In general, these depend upon the nature of the equipment and the data objectives of the satellite. The requirement that the satellite be injected in daylight adds horizontal lines of constraint to the map (Reference 17). Constraints on the maximum and minimum spin-axis sun angles add sliding lines (parallel to the node lines).

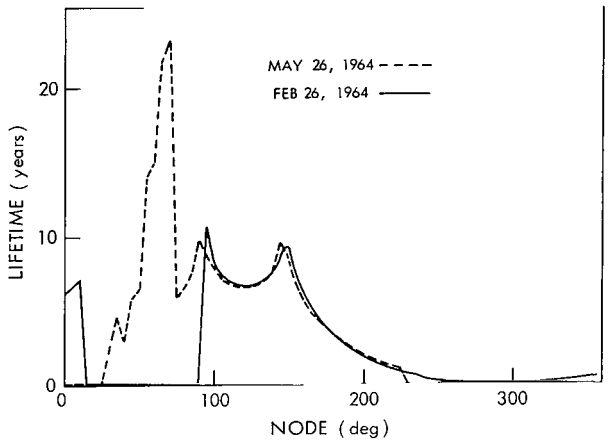


Figure 28—Lifetime vs. node for IMP.

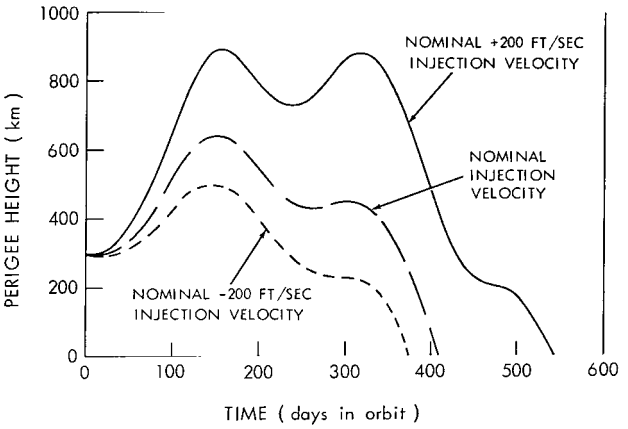


Figure 29—Effect of a change in the initial velocity on the lifetime of the S-3 orbit. The assumed launch date is August 7, 1962 and $\Omega_0$ = 206 deg.

## Gravitational Kill

The problem of controlling the lifetime of a satellite was investigated to determine whether this would provide a feasible method of limiting the radio transmission of an S-3 satellite. The results show: (1) an error of 200 ft/sec in the injection speed will cause an uncertainty of about 100 days in the lifetime; (2) computational differences between the ITEM and Halphen methods are insignificant in determining the lifetime; and (3) differences in lifetime for different days within a 2 month period, with the node constant, are about 2 or 3 months.

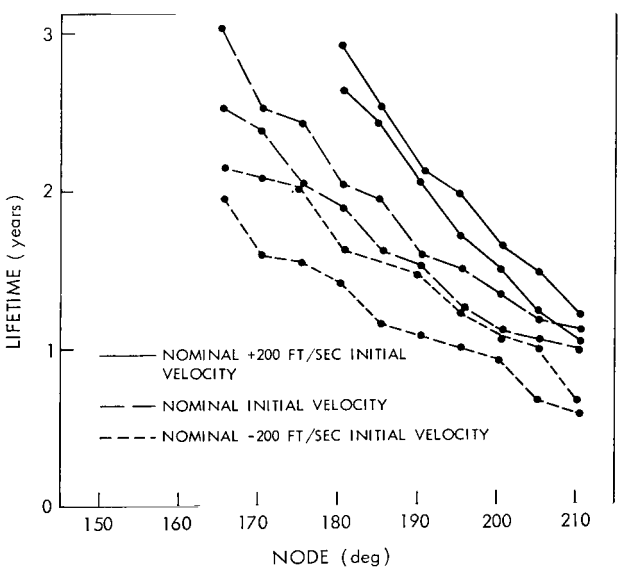


Figure 30—Lifetime vs. node for S-3. The upper lines indicate the times when perigee reaches the ground. The lower lines indicate the times when perigee reaches 300 km. The Halphen method is used and only gravitational forces are considered.

When the injection speed is varied within the tolerances, the qualitative behavior of the perigee rise remains the same during the desired lifetime of a year or two. The actual behavior of perigee for 1 value of node as a function of injection speed is shown in Figure 29. The second amplitude in perigee height is smaller than the first for the nominal and nominal - 200 ft/sec orbits, apparently because the oblateness causes a more rapid rotation of the line of apsides, moving it away from an upward trend.

The results are summarized on a chart (Figure 30) of lifetime vs. node (dots represent computed points.) The minimum lifetime for each case was considered to be the time when

perigee reaches 300 km; the maximum lifetime when the perigee was at ground level. The more precise criterion that the fall time is when perigee reaches 120 km may be used (Figure 18). However, the assumed error in the injection speed gives much more spread in the lifetime.

## ACKNOWLEDGMENTS

The author wishes to acknowledge the help of her colleagues who monitored this work and reviewed the paper, and J. A. Chiville and K. T. Shuey who prepared many of the graphs.

(Manuscript received May 19, 1964)

REFERENCES

1. Kaula, W. M., "A Review of Geodetic Parameters," NASA Technical Note D-1847, May 1963, p. 1.
2. "The American Ephemeris and Nautical Almanac for the Year 1964," Washington: U.S.Government Printing Office, 1962, p. 10.
3. Wolf, H., Shaffer, F., and Squires, R. K., "Interplanetary Trajectory Encke Method (ITEM) Program Manual," Goddard Space Flight Center Rept. X-640-63-71 May 1963.
4. Musen, P., "A Discussion of Halphen's Method for Secular Perturbations and its Application to the Determination of Long Range Effects in the Motions of Celestial Bodies, Part I," NASA Technical Report R-176, 1963.
5. Harris, I., and Priester, W., "Theoretical Models for the Solar-Cycle Variation of the Upper Atmosphere," NASA Technical Note D-1444, August 1962.
6. O'Keefe, J. A. Eckels, A., and Squires, R. K., "The Gravitational Field of the Earth," *Astronom. J.*64(7):245-253, September 1959
7. Kozai, Y., "On the Effects of the Sun and the Moon Upon the Motion of a Close Earth Satellite," Smithsonian Astrophys. Observ. Spec. Rept. 22:7-10, Cambridge, Mass., March 20, 1959.
8. Musen, P., Bailie, A., and Upton, E., "Development of the Lunar and Solar Perturbations in the Motion of an Artificial Satellite, " NASA Technical Note D-494, January 1961, p. 40.
9. Shute, B. E., "A Cislunar Orbit (IMP)," *Astronom. J.* 67(5):283, June 1962 (abstract).
10. Moe, M. M., "Solar-Lunar Perturbations of the Orbit of an Earth Satellite," *ARS* 30(5):485-487, May 1960.
11. Brouwer, D., and Clemence, G. M., "Methods of Celestial Mechanics," New York: Academic Press, 1961, pp. 253-260.

12. Kozai, Y., "Secular Perturbations of Asteroids with High Inclination and Eccentricity," *Astronom. J.*67(9):591-598, November 1962.

13. Kozai,Y., "The Earth's Gravitational Potential Derived from the Motion of Satellite 1958 Beta Two," Smithsonian Astrophy. Observ. Rept. 22:1-6, Cambridge, Mass., March 20, 1959.

14. Moulton, F. R., "An Introduction to Celestial Mechanics," 2d rev. ed., New York: The Macmillan Company, 1914, p. 332.

15. Whitney, C. A., "The Structure of the High Atmosphere," Smithsonian Institution Astrophysical Observatory, Special Rept. 25, April 20, 1959.

16. Minzer, R. A., and Ripley, W. S., "The ARDC Model Atmosphere, 1956," Air Force Cambridge Research Center, Bedford, Mass, Document TW-56-204, and Armed Forces Technical Information Agency, Dayton, Ohio Document 110233, December 1959.

17. Montgomery, H. E., and Paddack, S. J., "S-49, EGO Launch Window and Orbit," Goddard Space Flight Center Rept. X-640-63-119, July 1963, Figure 5.

*"The aeronautical and space activities of the United States shall be conducted so as to contribute . . . to the expansion of human knowledge of phenomena in the atmosphere and space. The Administration shall provide for the widest practicable and appropriate dissemination of information concerning its activities and the results thereof."*

—NATIONAL AERONAUTICS AND SPACE ACT OF 1958

# NASA SCIENTIFIC AND TECHNICAL PUBLICATIONS

TECHNICAL REPORTS: Scientific and technical information considered important, complete, and a lasting contribution to existing knowledge.

TECHNICAL NOTES: Information less broad in scope but nevertheless of importance as a contribution to existing knowledge.

TECHNICAL MEMORANDUMS: Information receiving limited distribution because of preliminary data, security classification, or other reasons.

CONTRACTOR REPORTS: Technical information generated in connection with a NASA contract or grant and released under NASA auspices.

TECHNICAL TRANSLATIONS: Information published in a foreign language considered to merit NASA distribution in English.

TECHNICAL REPRINTS: Information derived from NASA activities and initially published in the form of journal articles.

SPECIAL PUBLICATIONS: Information derived from or of value to NASA activities but not necessarily reporting the results of individual NASA-programmed scientific efforts. Publications include conference proceedings, monographs, data compilations, handbooks, sourcebooks, and special bibliographies.

***Details on the availability of these publications may be obtained from:***

**SCIENTIFIC AND TECHNICAL INFORMATION DIVISION**

**NATIONAL AERONAUTICS AND SPACE ADMINISTRATION**

**Washington, D.C. 20546**